Finite Temperature Behavior of Gas Phase Neutral Aun (3 ≤ n ≤ 10) Clusters: A First Principles Investigation

4 AUTHORS, INCLUDING:

Sailaja Krishnamurty
Central Electrochemical Research Institute
54 PUBLICATIONS **885** CITATIONS

SEE PROFILE

Sourav Pal
CSIR - National Chemical Laboratory, Pune
**180** PUBLICATIONS **2,823** CITATIONS

SEE PROFILE

Finite Temperature Behavior of Gas Phase Neutral Au$_n$ (3 ≤ n ≤ 10) Clusters: A First Principles Investigation

Himadri Sekhar De,[†] Sailaja Krishnamurty,*,[‡] Deepti Mishra,[†] and Sourav Pal*,[†]

[†]Theoretical Chemistry Group, Physical Chemistry Division, National Chemical Laboratory, Pune-411 008, India
[‡]Functional Materials Division, Central Electrochemical Research Institute, Karaikudi-630 006, India

ABSTRACT: Relativistic density functional theory (DFT) based molecular dynamical simulations are performed on gold clusters with 3—10 atoms (Au$_n$, n = 3—10) with an aim of understanding their finite temperature behavior. Conformations of a cluster coexisting at different temperatures are analyzed. The simulations reveal that the finite temperature behavior of Au clusters can be classified into three regions, viz., a "solid-like" region, a "structural fluctionality" region, and a "liquid-like" state. The structural fluctionality region is when the cluster dynamically interconverts between two conformations through a metastable intermediate.

For Au$_n$, n ≤ 7, where the atoms reorient continuously such that two planar conformations coexist. On the other hand, for Au$_n$, n ≥ 8, the cluster behaves as a quasi-planar liquid where the outer edge atoms of the cluster bend and relax alternatively around a central planar region. In liquid-like state the cluster is predominantly in a 3D conformation and transits through various conformations. The onset and duration of each of the above three regions are seen to be size dependent. Au$_6$ is the most stable cluster and remains in its ground state conformation (or solid-like region) up to nearly 1100 K. Au$_9$ is the least stable among the studied clusters with a liquid-like state around room temperature itself. All the clusters with the exception of Au$_6$ enter the liquid-like state at much lower temperatures as compared to that of bulk gold.
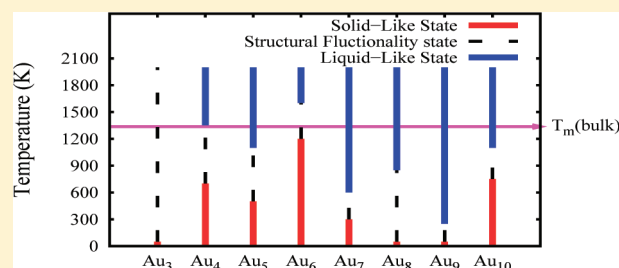
I. INTRODUCTION

With respect to the bulk and atomic scale chemistry, the gas phase chemistry of metal clusters is surprisingly different. One of the most important features is their higher catalytic activity as compared to that of bulk.[1,2] This along with the other notable features such as electronic transport,[3,4] magnetic,[5,6] and optical properties[7,8] have led to a surge in the research activity on them. This is especially the case for clusters comprising 2—50 atoms (also referred to as zero dimensional quantum dots) where the quantum confinement of electrons results in size specific physical and chemical properties.

These research works have established that clusters at finite temperatures undergo a physical transformation (phase transformation) from a "solid-like" state to a "liquid-like" state. At low temperatures, the atoms in a cluster vibrate around their equilibrium positions similar to the case of a bulk solid and hence the name solid-like state. As the temperature increases, atoms in the clusters diffusively reorient their equilibrium positions and transform into other minimum energy conformations. At much higher temperatures, these transitions are observed to happen at higher frequencies (i.e., transits through several conformations in a few femtoseconds). These conformational reorientations/isomerization increases dramatically beyond a temperature specific to each cluster after which the cluster begins to resemble a liquid droplet and hence the name liquid-like state. This phenomenon has been widely explored in several clusters such as silicon,[9]

gallium,[10] aluminum,[11] tin,[12] sodium,[13] and gold[14] using experimental and/or theoretical methods.

From the chemical point of view, small clusters have highly active coordination sites for catalytic activity unlike periodic surfaces, which makes them more important, apart from the above-discussed physical features. These sites and their activities vary with size and shape of the cluster. The catalytic reactions on these sites occur at various finite temperatures.[15] Due to isomerization discussed above, there is an observable correlation between the shape of the cluster and its temperature. Following this, the type and the number of surface reactive sites available for a reacting molecule (in other words, the cluster's functional catalytic activity) are modified. Hence, stability of a given geometry or an understanding of different isomers coexisting for a cluster at its working temperature is significant. This information is lacking in the literature and hence a limitation in its practical applications.

In this context, the catalytic properties of Au clusters have been the most prominent. Hence, the potential energy surface of Au$_n$ (4 ≤ n ≤ 15) has been the most studied topic using theoretical,[16] experimental,[17] and a combination of both these methods.[18] One of the reports using photoelectron spectroscopy (PES) demonstrates the possibility of liquid-like states coexisting

for Au$_7$ when generated at 100 K.[19] Along the same lines, Wang and co-workers using PES and density functional theory (DFT) have demonstrated the coexistence of several planar isomers in Au$_{10}^-$ and Au$_{12}^-$.[20] Studies using ion mobility spectrometry and trapped electron diffraction propose that there is a coexistence of several isomers at room temperature[21] in cationic and anionic Au$_n$ ($n \leq 9$) clusters. The existence of this liquid-like state is also validated by a debate on 2D−3D (two-dimensional−three-dimensional) transition within the Au clusters.[22] Apart from the above-mentioned few works, stability and various isomers present at a given working temperature of Au clusters is not well explored experimentally.

Theoretically, the finite temperature property/behavior of intermediate sized gold clusters has been investigated by a few groups using classical MD simulations.[23] One such report[24] mentions that Au clusters with 13−2869 atoms undergo a phase transition between 600 and 750 K. In another work, Cleveland et al. using an embedded atom potential show that the Au$_n$ ($n < 250$) clusters undergo a solid (from a low temperature structure) to solid transformations (an icosahedral, I_h structure) before a solid-like to liquid-like transformation around 760 K.[25] One of the interesting conclusions on the Au cluster dynamics using classical mechanics based methods is that surface mobility of atoms within the Au clusters enhances their catalytic activity from 300 K onward. BOMD was also applied to a limited extent to study the finite temperature behavior of Au clusters.[14,26,27]

However, the most interesting point raised so far is by Moseler and co-workers, who have reported a coexistence of two hetero-dimensional phases (a free planar Au liquid phase which coexists with the usual three-dimensional liquid) in anionic Au$_n$ ($11 \leq n \leq 14$) clusters from tight binding DFT simulations.[27] Their work has further emphasized on the complications in validating the theoretically proposed ground state geometries. Thus, there seems to exist a more complex potential energy surface within Au clusters, with several conformations coexisting (the coexistence is likely to be more pronounced with increasing cluster size) at various working temperatures.

In light of the above discussion, in the present work, we explore the finite temperature behavior/thermodynamic stability of neutral gas phase Au clusters with 3−10 atoms (Au$_n$, $n = 3$−10). In this range, due to their planarity, the Au clusters are proposed to be highly reactive.[28] Further, all the atoms in this size range are surface atoms. For this purpose, we have carried out ab initio molecular dynamical simulations on Au$_n$, $n = 3$−10, clusters at various temperatures. From the simulations, we discuss the geometrical rearrangements of atoms within different sized and shaped clusters.

The paper is organized as follows. In section II, we discuss the computational methodology and clusters for which the simulations are carried out. In section III, we note the results from the simulation studies. Section IV discusses the implication of various molecular dynamical results reported in section III. We conclude the work in brief in section V.

II. COMPUTATIONAL DETAILS

All calculations are performed in the framework of density functional theory (DFT), using a linear combination of Gaussian orbitals as implemented in deMon2k code.[29] Several conformations are generated for each cluster size. All such generated conformations are optimized using the Perdew−Burke−Ernzerhof (PBE) exchange and correlation functional[30] with 1997 Stuttgart−Dresden Relativistic Effective Core Potentials (RECPs)[31] as the basis set for the valence electrons. 5s, 5p, 5d,
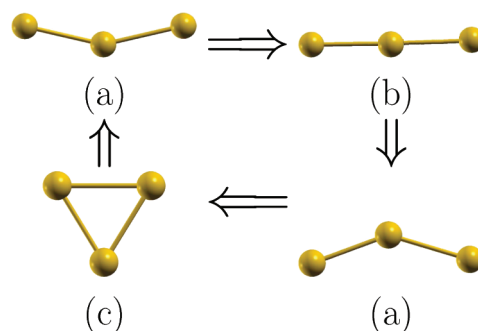
Figure 1. Cycle of conformational reorientation observed in Au$_3$ cluster between 200 and 2000 K.

and 6s electrons are considered to constitute the valence electrons. We note that these ECPs are now documented for the accurate prediction of structure as well as spectroscopic properties of Au clusters.[32,33] No additional polarization functions are added. The A2 auxiliary functions are used to fit the charge density.[34] The convergence of the geometries is based on gradient and displacement criteria with a threshold value of 10^{-5} au and the criteria for convergence of an SCF cycle was set to 10^{-9}. Only the lowest spin state is considered for all the Au clusters. Thus, the spin multiplicity for an even electron (even number of Au atoms) cluster is singlet and doublet for odd electron (odd number of Au atoms) clusters. It has also been reported earlier that Au clusters prefer to be in their lowest spin state.[35] Following the geometry optimization, harmonic vibrational frequencies are computed for various conformations of Au$_n$ ($3 \leq n \leq 10$). All of the frequencies are found to be positive, thereby indicating the conformations to be a local minima.

The lowest energy conformation is chosen as the starting conformation for all of the molecular dynamical (MD) simulations. The finite temperature simulation for each cluster is carried out implementing Born−Oppenheimer molecular dynamics (BOMD) using the same exchange-correlation functionals and RECPs as described above. The simulations are carried out between 200 and 2000 K. At each temperature, the cluster is equilibrated for a time period of 10 ps followed by a simulation time of 30 ps. The temperature of the cluster is maintained using Berendsen's thermostat ($\tau = 0.5$ ps). The nuclear positions are updated using a velocity Verlet algorithm with a time step of 1 fs. The atomic positions and bond length fluctuations of atoms are analyzed using traditional parameters such as root mean square bond length fluctuations (δ_{rms}) and the mean square ionic displacements (MSDs). The δ_{rms} is defined as

$$\delta_{rms} = \frac{2}{N(N-1)} \sum_{i<j} \frac{\sqrt{\langle R_{ij}^2 \rangle_t - \langle R_{ij} \rangle_t^2}}{\langle R_{ij} \rangle_t} \quad (1)$$

where N is the number of particles in the system, r_{ij} is the distance between the ith and jth particle in the system and $\langle ... \rangle_t$ denotes a time average over the entire trajectory. The MSD of an individual atom is defined as

$$\langle R_i^2 \rangle = \frac{1}{M} \sum_{m=1}^{M} [R_i(t_{0m} + t) - R_i(t_{0m})]^2 \quad (2)$$

where $R_i(t_{0m})$ is the instantaneous position of atom i at t_0 and $R_i(t_{0m} + t)$ is the corresponding position of atom i after a time interval t.
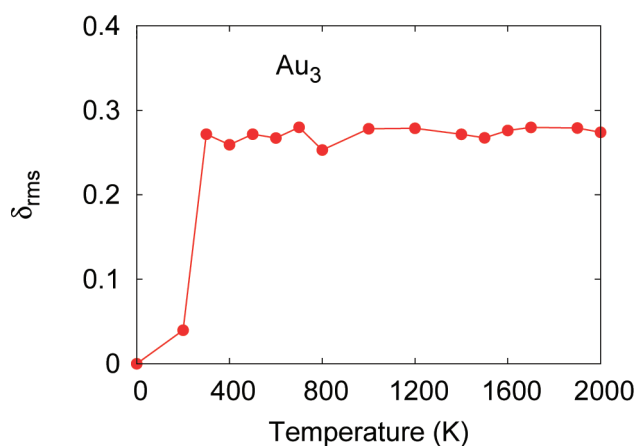
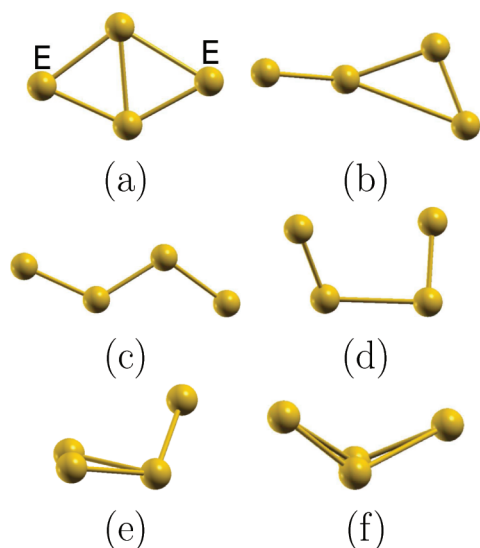**Figure 2.** δ_{rms} of Au$_3$ as a function of temperature.

Figure 4. δ_{rms} of Au$_4$. I, II, and III correspond to different states of a cluster as a function of temperature.

Figure 3. Various conformations of Au$_4$ observed during an MD simulation. (a) corresponds to the ground state conformation.

Figure 5. Various conformations seen during the MD simulation of Au$_5$. (a) corresponds to the ground state conformation.

III. RESULTS

A. Au$_3$. The cluster with three atoms is quite small with limited conformational reorientation available within. The ground state conformation of Au$_3$ is a bent structure with an Au—Au—Au angle of 162° (conformation shown as (a) in Figure 1). This conformation is nearly degenerate (the energy difference between both the conformations is just 0.3 kcal/mol) with that of a linear conformation shown as (b) in Figure 1. The simulations are carried out with bent structure as the starting conformation. An analysis of ionic motion around 200 K shows that the cluster evolves smoothly from the bent structure to the linear one and further to a triangular conformation (see Figure 1c). Incidentally, this triangular conformation is just 5 kcal/mol higher in energy with respect to the ground state conformation. Thus, even at a low temperature of 200 K, there is an evolution between all possible conformations within a three atom cluster. Around 200 K, the triangular conformation is an obtuse angle triangle with an Au—Au—Au angle reaching a minimum of 100° with respect to the linear conformation. At 300 K and above, the triangular
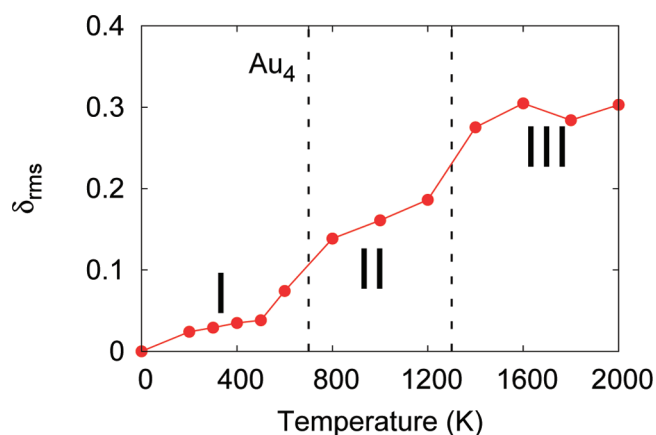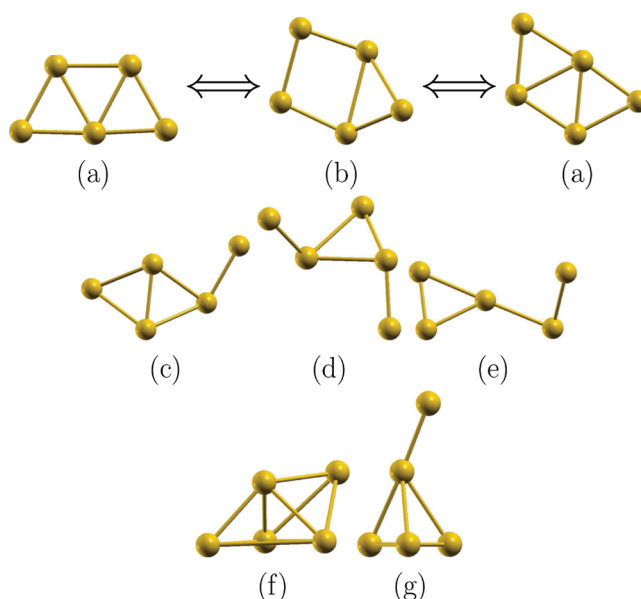
conformation is equilateral with all the bond angles around 60°. This is reflected clearly in the δ_{rms} plot shown in Figure 2. The value is lower for 200 K where the two end atoms of bent conformation come close enough to only form an obtuse angle triangle. Interestingly, the cluster does not dissociate even up to 2000 K, and the cluster undergoes a cyclic path of conformational reorientation between 200 and 2000 K as shown in Figure 1.

B. Au$_4$. The ground state geometry of Au$_4$ is a cyclic rhombus conformation shown in Figure 3a. MD simulations with this conformation as the starting geometry are carried out between 200 and 2000 K. On the basis of the conformational reorientation seen in Au$_4$, the behavior of the cluster can be classified into three regions/states. Region I is between 200 and 600 K, where atoms vibrate around their equilibrium position of the ground state conformation. Significantly, the two edge atoms (atoms indicated by E in Figure 3a) show higher displacements as compared to the central atoms of the ground state conformation. Region II is between 800 and 1200 K, where the cluster transits between
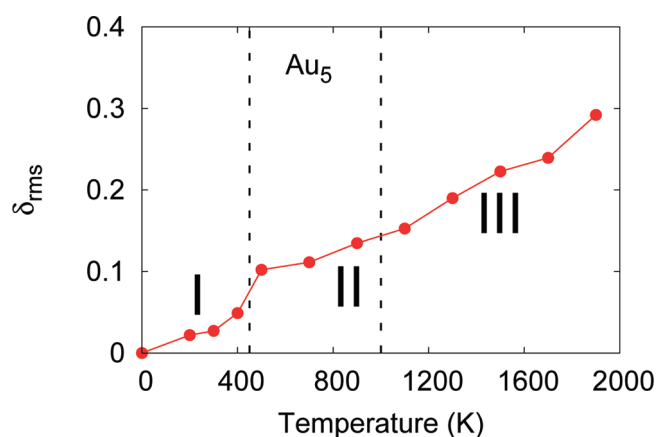
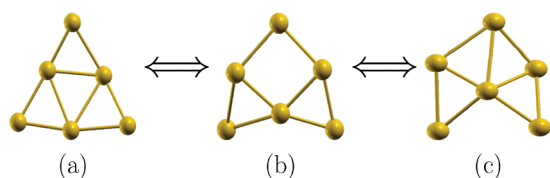**Figure 6.** δ_{rms} of Au$_5$ with various regions highlighted.

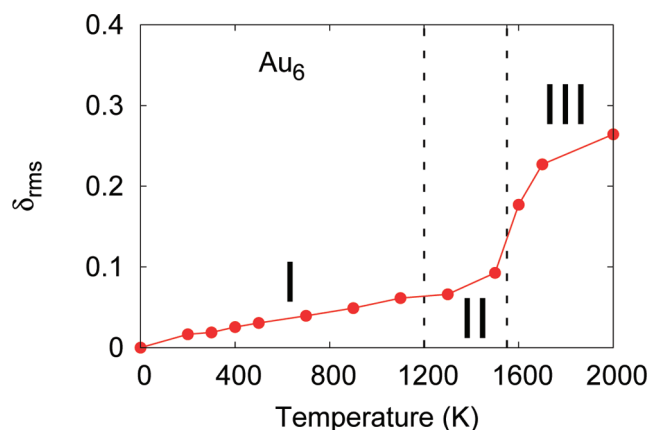**Figure 7.** Structural fluctionality observed in Au$_6$ between 1300 and 1500 K.

Figure 8. δ_{rms} for Au$_6$. The cluster retains its ground state conformation up to 1100 K.

Figure 9. Various conformations seen during the MD simulation of Au$_7$.
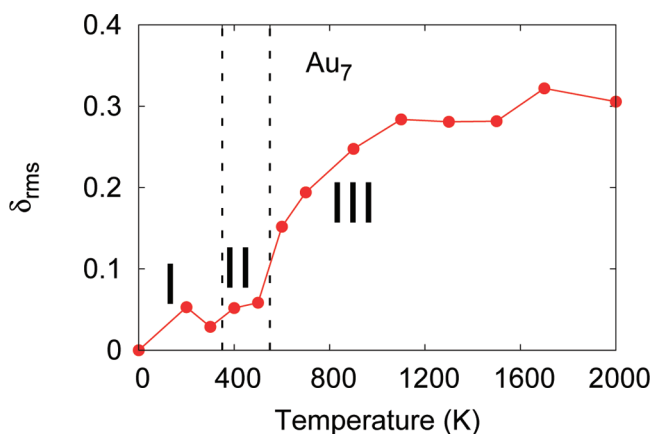
Figure 10. Root mean square (rms) displacement in Au$_7$.

ground state and next excited state conformation (see Figure 3b). During this transition, the dangling atom in Figure 3b bonds and dissociates in a cyclic fashion with alternating edges of the triangle. Such a transition from one conformation to another is more commonly referred to as structural fluctionality.[36] This can be also envisaged as a region of planar fluidity where, the cluster essentially retains its 2D orientation, while the dynamic movements of few significant atoms reorient the cluster into two or three different planar configurations. Region III is 1400 K and above, where the cluster frequents some high-energy planar conformations and 3D conformations in addition to the two conformations noted in the region II (see Figure 3c−f). This state is thus a liquid-like state. The above-mentioned ionic
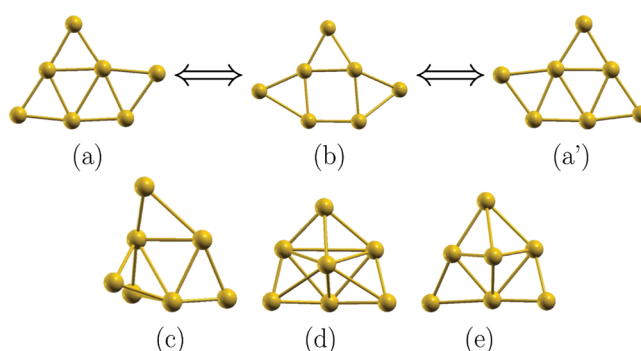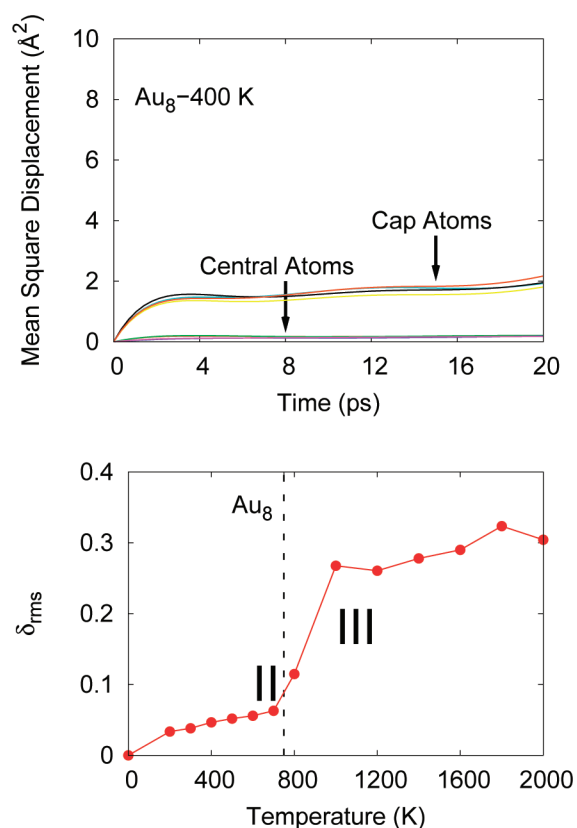
movements reflect in Figure 4. The δ_{rms} hovers around 0.03 between 200 and 600 K. It shows a linear increase between 600 and 1200 K where the cluster oscillates between the ground state and an excited state which is 0.32 kcal/mol above the ground state conformation. Other planar conformations which lie around 6−10 kcal/mol above the starting conformation are observed around 1400 K. Also it is only around this temperature that the atoms in the cluster diffuse enough to orient into 3D conformations. These conformations lie about 20 kcal/mol above the ground state conformation. One of the conformations shown in Figure 3f is a distorted T_d conformation. Thus, the Au$_4$ ground state conformation is seen to be stable up to at least 600 K. Interestingly, Na$_4$ also exhibits similar finite temperature behavior as Au$_4$.[37]

C. Au$_5$. The ground state geometry of Au$_5$ is an extension of Au$_4$, with an additional edge of a triangle being capped (see Figure 5a). As in the case of Au$_4$, the finite temperature behavior of the cluster can be classified into three regions, viz.: (a) A solid-like region where the atoms vibrate around their ground state region (from 200 to 400 K), called region I. (b) a planar liquid-like region, where the ground state transits through a metastable state (see Figure 5b) before returning back to its original configuration. This involves a rearrangement of the two cap atoms of the triangle between 500 and 1000 K. Thus, Au$_5$, like in case of Au$_4$ also exhibits structural fluctionality. (c) Around 1100 K, few high planar high energy conformations such as structures c and d of Figure 5 are seen. Above 1500 K, the 3D conformations are also seen. These conformations lie typically about 15−20 kcal/mol above the ground
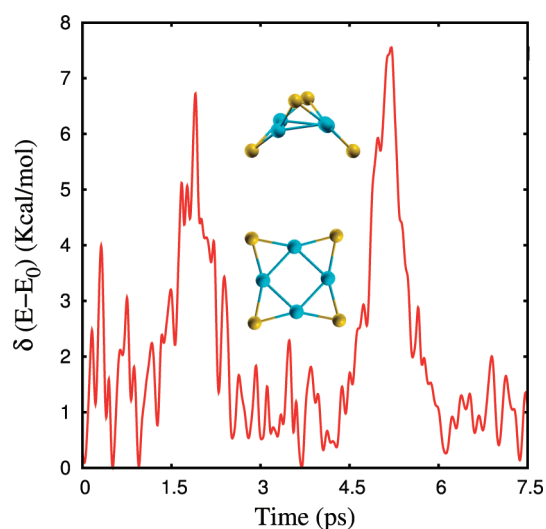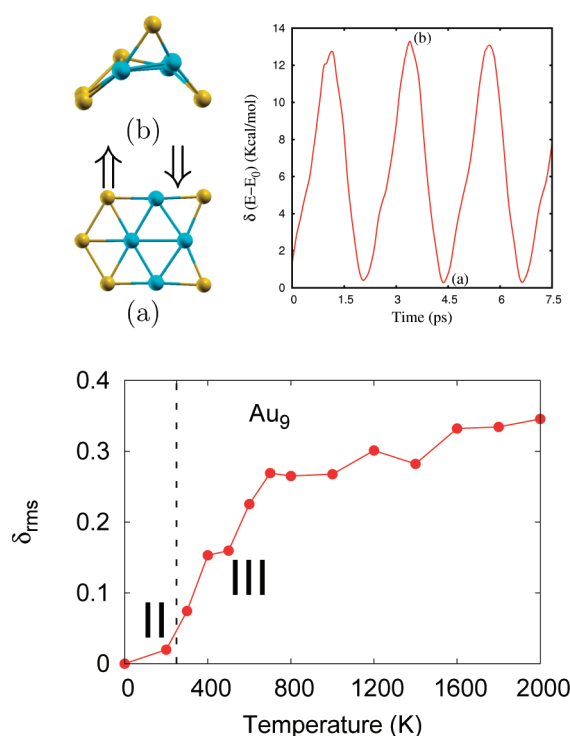
Figure 11. Oscillations in the potential energy (PE) given in kcal/mol for Au_8 at 200 K. Also shown are the two conformers corresponding to extrema in the PE. The four blue atoms correspond to the central plane. The rest of the atoms bend around this plane in a symmetric fashion.

Figure 12. MSD and δ_{rms} for Au_8 of individual atoms in Au_8 as seen at 400 K.

Figure 13. The two conformational orientations seen for Au_9 at 200 K. The atoms highlighted in blue correspond to the plane of atoms which vibrate around their equilibrium positions. The rest of the atoms undergo symmetric displacements about the plane. Also shown in the figure is the corresponding oscillation in the potential energy for (a) and (b) conformations. δ_{rms} for Au_9 is given below in the figure.

temperatures. Figure 8 gives the δ_{rms} for Au_6 cluster. An analysis of ionic motion shows that the atoms vibrate around their equilibrium positions in the ground state geometry up to a temperature of 1100 K. Above this temperature, the cluster undergoes a transition between the ground state planar structure and a next high energy planar conformation which is 7 kcal/mol higher in energy via a metastable conformation (shown as (b) in Figure 7). Interestingly, the same structural fluctionality seen above has been reported in one of the earlier works on Au_6^- cluster The report indicates this transition to have an energy barrier of nearly 9 kcal/mol.[15a] which is seen to be reduced by the chemical adsorption of various ligands. It is only around 1600 K that the cluster transforms into a liquid-like state where it transits through several high energy planar and 3D conformations. This temperature of 1700 K is remarkably high as compared to the melting temperature of bulk gold which is around 1337 K.

E. Au_7. The ground state geometry of Au_7 is a capped Au_6 conformation (see Figure 9a). The atoms in the cluster vibrate about their equilibrium positions in ground state conformation around 200 and 300 K. Around 400 and 500 K, the cluster shows a structural rearrangement from ground state geometry to a metastable conformation (see Figure 9b) before collapsing back into its mirror image (see Figure 9a'). At 600 K and above, the system enters a liquid-like state with the cluster visiting several 3D conformations shown in Figure 9c–e. Thus, the planar liquid-like region is quite small and limited to 400–500 K in Au_7. The various regions of cluster behavior are clearly demarcated in Figure 10.

state conformation. These atomic movements reflect in the root-mean-square displacement values plotted in Figure 6.

D. Au_6. The ground state geometry of Au_6 which corresponds to three capped edges of a triangle (see Figure 7a), is the most stable conformation among all the clusters studied with the cluster remaining in its ground state conformation up to considerably high
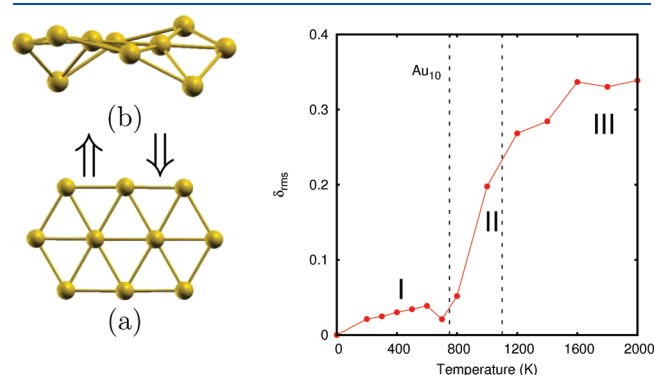
F. Au$_8$. The ground state geometry of Au$_8$ consists of a square with each of its edges capped by an Au atom.[33] An analysis of the ionic motion around 200 K reveals a slightly different behavior as compared to clusters discussed so far. The four cap atoms bend around the central square in a symmetric fashion. This is more clearly understood from Figure 11. The figure demonstrates the fluctuations within potential energy with the ground state conformation referenced as zero. During the course of simulation the potential energy increases in spikes of ~6−7 kcal/mol. During these increments, the cluster gets enough kinetic energy and the cap atoms bend around the plane of the central atoms. These distortions are very symmetric with the two diagonally placed caps bending downward and the other two bending upward. Figure 12 gives the individual mean square displacements of atoms from their equilibrium positions, and this clearly shows that while the central four atoms are more rigid and remain very close to their equilibrium positions, the cap atoms undergo larger displacements. This behavior extends up to 700 K with the cap atoms undergoing the displacement with increasing frequency and amplitude as a function of temperature. Around 800, the additional 3D conformations are seen. At 900 K and above, the cluster begins to resemble a liquid droplet transiting through several 3D conformations in addition to the ground state conformation and other planar conformations. This transition is clearly seen from δ_{rms} in Figure 12.

G. Au$_9$. Au$_9$ ground state geometry, being a growth over Au$_8$, is seen to be quite unstable. Around 200 K, the ground state geometry undergoes a structural fluctionality as in case of Au$_8$ as shown in Figure 13. However, above 300 K, the cluster is seen to transit through various high energy planar and other nonplanar conformations. Thus, the cluster already begins to resemble a liquid droplet. The cluster is in a complete liquid-like state by 600 K as is clearly seen from the δ_{rms} plot in the Figure 13.
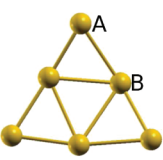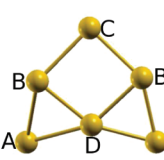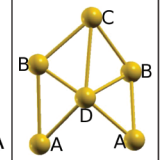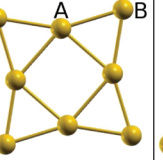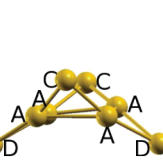
H. Au$_{10}$. Au$_{10}$ ground state geometry is stable up to 700 K with the atoms vibrating about their equilibrium positions. Around 800 K, the cluster undergoes constrained deformation about the plane of the cluster as shown in Figure 14. Above 1000 K, the cluster transits through several 3D conformations in addition to several excited state planar conformations thereby resembling a liquid state system.
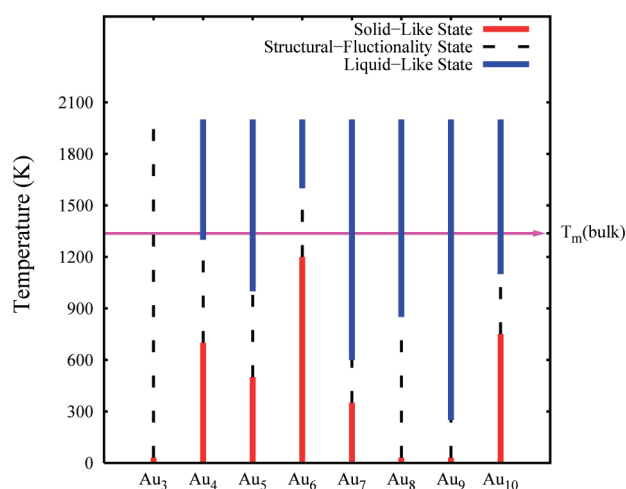
IV. DISCUSSION ON THE FINITE TEMPERATURE BEHAVIOR OF AU$_N$ (N = 3−10) CLUSTERS

Traditionally, clusters are known to transit from a solid-like state and a liquid-like state as a function of temperature. Each of these states has their own significance. The solid-like region/state is significant due to the structural stability and an assurance of a constant electronic and geometric configuration. This state is important for applications where the clusters are applied for their response properties, which are size and shape sensitive. The liquid-like state is a more dynamic state, which is significant during the synthesis of bigger nanoparticles where a soft electronic and geometric structure is needed. Interestingly, all the gold clusters studied in the present work exhibit a structural rearrangement state (where they transit through two or three isomers) before they enter into a liquid-like state.

Table 1 shows the conformations in Au$_6$ and Au$_8$ clusters respectively and the Lowdin charge distribution on them as they undergo the above structural rearrangement. It is clearly evident from the values in the table that a structural rearrangement is accompanied by a moderate to considerable charge redistribution. For example, site A in Au$_6$ undergoes a significant charge depletion, while the site C (which is site A before the structural change) gains some charge. When a ligand molecule such as CO is adsorbed on site B through carbon atom, the presence of a more negatively charged C site adjacent to it will help in an easier reduction process of it. Similar analysis can be drawn for other ligand molecules such as O$_2$, CH$_3$OH, etc. In the case of Au$_8$ also there is some charge redistribution leading to more negatively and positively charged atoms. Thus, the cluster is more polarized during the process. Hence, the presence such a structural rearrangement appears to be important for many catalytic reactions

Figure 14. The conformational orientation seen in Au$_{10}$ between 800 and 1000 K (region II). Also shown in the figure is the δ_{rms} for Au$_{10}$.

Table 1. Lowdin Population Analysis for Various Conformations Observed in Au$_6$ between 1100 and 1600 K and in Au$_8$ between 200 and 800 K

Cluster Reactivity Site	Au$_6$(a)	Au$_6$(b)	Au$_6$(c)	Au$_8$(a)	Au$_8$(b)
A	-0.164	-0.120	-0.070	-0.173	-0.185
B	0.165	0.151	0.144	0.173	–
C	–	-0.150	-0.259	–	0.183
D	–	0.133	0.103	–	0.186

Figure 15. Summary of various thermodynamic states within Au_n clusters. The arrow indicates the melting temperature of bulk gold (T_m (bulk)).
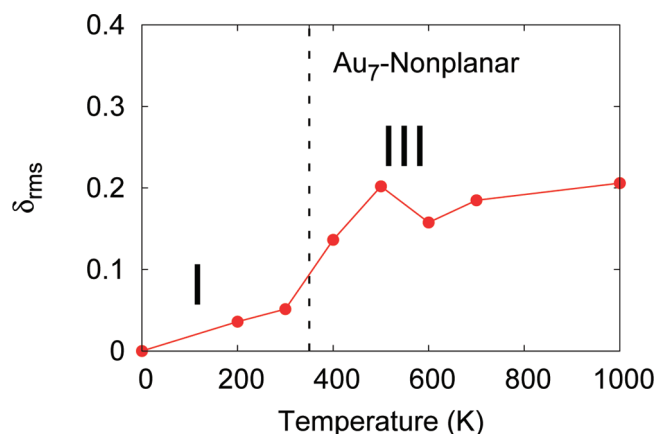
Figure 16. δ_{rms} of Au_7 with nonplanar conformation as starting geometry.

where the atoms need to reorient with a modified charge distribution on adsorption of ligands. This facilitates the oxidation and reduction reaction mechanisms to have a lower barrier. Similar significance of this structural rearrangement is also proposed by other experimental and theoretical studies.[36,38]

In Figure 15, we summarize the observed finite temperature behavior of Au_n ($n = 3-10$) clusters. The figure clearly shows that Au_3, Au_8, and Au_9 clusters do not exhibit a solid-state-like behavior even at low temperatures. On the other hand, Au_6 is stable up to nearly 1100 K, highest among all the clusters studied. In general, it can be commented that the "solid-like" region is comparatively larger for clusters with even atoms. The structural fluctionality region is comparatively large for Au_8 and Au_3.

In order to understand the significance of this structural rearrangement in the case of different starting conformations, we have carried out a BOMD simulation with a nonplanar isomer of Au_7 as the starting conformation. This isomer is reported to coexist along with the planar conformations in the recent experimental and theoretical reports.[19,33] An analysis of the ionic motion as a function of temperature in this simulation clearly shows that the finite temperature behavior of this conformation can be clearly divided into solid-like and liquid-like states.

The regions are demarcated and shown in Figure 16. The atoms in the cluster vibrate around their equilibrium positions up to 300 K. At 400 K and above the cluster visits several other high-energy 3D conformations along with few planar conformations. This was found to be consistently true in the case of BOMD simulations with a nonplanar conformation as the starting geometry in Au_8 as well as Au_9. Thus, the structural fluctionality/rearrangement appears to be characteristic of planar Au conformations. This behavior is probably an explanation of the higher catalytic activity of the small planar Au clusters[39] in comparison to their nonplanar conformations.

V. CONCLUSIONS

Born—Oppenheimer molecular dynamical simulations on Au_n ($n = 3-10$) reveal a size-dependent finite temperature behavior of clusters. The study shows that in clusters such as Au_3, Au_8, and Au_9 more than one isomer may coexist at 300 K. Au_6 is the most stable conformation with only the ground state conformation dominating up to nearly 1100 K. A dynamic transition between two isomers or two conformations is observed in all the clusters between the solid-like state and liquid-like state. Such a fluction-ality is seen to be size-specific and characteristic of planar conformations in this study. This transition called thermally driven structural fluctionality may be quite significant and contribute positively to catalytic property of the planar gold clusters.

■ AUTHOR INFORMATION

Corresponding Authors
*E-mail: Sourav Pal, s.pal@ncl.res.in; Sailaja Krishnamurty, sailaja.raaj@gmail.com.

■ ACKNOWLEDGMENT

■ REFERENCES

(1) (a) Haruta, M.; Yamada, N.; Kobayashi, T.; Iijima, S. *J. Catal.* **1989**, *115*, 301. (b) Hashmi, A. S. K. *Gold Bull.* **2003**, *36*, 3.

(2) (a) Hutchings, G. J. *J. Catal.* **1985**, *96*, 292. (b) Teles, J. H.; Brode, S.; Chabanas, M. *Angew. Chem.* **1998**, *110*, 1475.

(3) Yu, J.-X.; Chen, X.-R.; Sanvito, S. *Phys. Rev. B* **2010**, *82*, 085415.

(4) (a) Torma, V.; Vidoni, O.; Simon, U.; Schmid, G. *Eur. J. Inorg. Chem.* **2003**, 1121. (b) Clarke, L.; Wybourne, M. N.; Yan, M.; Cai, S. X.; Keana, J. F. W. *Appl. Phys. Lett.* **1997**, *71*, 617.

(5) (a) Li, X.; Kiran, B.; Cui, Li-Feng; Wang, L.-S. *Phys. Rev. Lett.* **2005**, *95*, 253401. (b) Pundlik, S. S.; Kalyanaraman, K.; Waghmare, U. V. *J. Phys. Chem. C* **2011**, *115*, 3809.

(6) Sessoli, R.; Gatteschi, D.; Caneschi, A.; Novak, M. A. *Nature* **1993**, *365*, 141.

(7) Pyykko, P. *Inorg. Chim. Acta* **2005**, *358*, 4113.

(8) Li, Q.; Wu, K.; Wei, Y.; Sa, R.; Cui, Y.; Lu, C.; Zhu, J.; He, J. *Phys. Chem. Chem. Phys.* **2009**, *11*, 4490.

(9) Krishnamurty, S.; Joshi, K.; Kanhere, D. G.; Blundell, S. A. *Phys. Rev. B* **2006**, *73*, 045419.

(10) (a) Breaux, G. A.; Cao, B.; Jarrold, M. F. *J. Phys. Chem. B* **2005**, *109*, 16575. (b) Breaux, G. A.; Hillman, D. A.; Neal, C. M.; Benirschke, R. C.; Jarrold, M. F. *J. Am. Chem. Soc.* **2004**, *126*, 8628.

(11) (a) Breaux, G. A.; Neal, C. M.; Cao, B.; Jarrold, M. F. *Phys. Rev. Lett.* **2005**, *94*, 173401. (b) Bagrets, A.; Werner, R.; Evers, F.; Schneider, G.; Schooss, D.; Wolfle, P. *Phys. Rev. B* **2010**, *81*, 075435.

(12) Shvartsburg, A. A.; Jarrold, M. F. *Phys. Rev. Lett.* **2000**, *85*, 2530.

(13) Schmidt, M.; Kusche, R.; von Issendorff, B.; Haberland, H. *Nature* **1998**, *393*, 238.

(14) Krishnamurty, S.; Shafai, G. S.; Kanhere, D. G.; Soule de Bas, B.; Ford, M. J. *J. Phys. Chem. A* **2007**, *111*, 10769.

(15) (a) Lang, S. M.; Bernhardt, T. M.; Barnett, R. N.; Yoon, B.; Landman, U. *J. Am. Chem. Soc.* **2009**, *131*, 8939. (b) Cox, D. M.; Brickman, R. O; Creegan, K.; Kaldor, A. *Mater. Res. Soc. Symp. Proc.* **1991**, *206*, 43. (c) Sun, Q.; Jena, P.; Kim, Y. D.; Fischer, M.; Gantefor, G. *J. Chem. Phys.* **2004**, *120*, 6510.

(16) (a) Xiao, L.; Tollberg, B.; Xiankui, B.; Wang, L. *J. Chem. Phys.* **2006**, *124*, 114309. (b) Chen, G.; Wang, Q.; Sun, Q.; Kawazoe, Y.; Jena, P. *J. Chem. Phys.* **2010**, *132*, 194306. (c) Shi, Y.-K.; Li, Z.-H.; Fan, K.-N. *J. Phys. Chem. A* **2010**, *114*, 10297.

(17) Hakkinen, H.; Landman, U. *Phys. Rev. B* **2000**, *62*, R2287.

(18) (a) Lechtken, A.; Schooss, D.; Stairs, J. R.; Blom, M. N.; Furche, F.; Morgner, N.; Kostko, O.; von Issendroff, B.; Kappes, M. M. *Angew. Chem., Int. Ed.* **2007**, *46*, 2944. (b) Walter, M.; Frondelius, P.; Honkala, K.; Hakkinen, H. *Phys. Rev. Lett.* **2007**, *99*, 096102. (c) Hockendorf, R. F.; Cao, Y.; Bayer, M. K. *Organometallics* **2010**, *29*, 3001. (d) Iwasa, T.; Nobusada, K. *J. Phys. Chem. C* **2007**, *111*, 45. (e) Shao, N.; Huang, W.; Gao, Y.; Wang, L.-M.; Lim, X.; Wang, L-S; Zeng, X. C. *J. Am. Chem. Soc.* **2010**, *132*, 6596. (f) Glib, S.; Weis, P.; Furche, F.; Ahlrichs, R.; Kappes, M. M. *J. Chem. Phys.* **2002**, *116*, 4094.

(19) Gruene, P.; Rayner, D. M.; Redlich, B.; Van der Meer, A. F. G.; Lyon, J. T.; Meijer, G.; Fielicke, A. *Science* **2008**, *321*, 674.

(20) (a) Wang, L.-M.; Pal, R.; Huang, W.; Zeng, X. C.; Wang, L.-S. *J. Chem. Phys.* **2010**, *132*, 114306. (b) Huang, W.; Wang, L.-S. *Phys. Rev. Lett.* **2009**, *102*, 153401.

(21) Schooss, D.; Weis, P.; Hampe, O.; Kappes, M. M. *Philos. Trans. R. Soc., A* **2010**, *368*, 1211.

(22) (a) Olson, R. M.; Vargonov, S.; Gordon, M. S.; Metiu, H.; Chretien, S.; Piecuch, P.; Kowalski, K.; Kucharski, S. A.; Musial, M. *J. Am. Chem. Soc.* **2005**, *127*, 1049. (b) Walker, A. V. *J. Chem. Phys.* **2005**, *122*, 94310. (c) Remacle, F.; Kryachko, E. S. *J. Chem. Phys.* **2005**, *122*, 44304. (d) Gronnbeck, H.; Broqvist, P. *Phys. Rev. B* **2005**, *71*, 073408. (e) Yuan, D. W.; Wang, Y.; Zeng, Z. *J. Chem. Phys.* **2005**, *122*, 114310.

(23) (a) Chushak, Y.; Bartell, L. S. *Eur. Phys. J. D* **2001**, *16*, 43. (b) Wang, Y.; Rashkeev, S. N. *J. Phys. Chem. C* **2009**, *113*, 10517. (c) Wang, Y.; Teitel, S.; Dellago, C. *J. Chem. Phys.* **2005**, *122*, 214722. (d) Cleveland, C. L.; Luedtke, W. D.; Landman, U. *Phys. Rev. B* **1999**, *60*, 5065.

(24) Gomez, J. C. R.; Rincon, L. *Rev. Mex. Fis.* **2007**, *53*, 208.

(25) Cleveland, C. L.; Luedtke, W. D.; Landman, U. *Phys. Rev. Lett.* **1998**, *81*, 2036.

(26) (a) Soule de Bas, B.; Ford, M. J.; Cortie, M. B. *J. Phys: Condens. Matter* **2006**, *18*, 55. (b) Chandrachud, P.; Joshi, K.; Krishnamurty, S.; Kanhere, D. G. *Pramana* **2009**, *72*, 845.

(27) Koskinen, P.; Hakkinen, H.; Huber, B.; von Issendorff, B.; Moseler, M. *Phys. Rev. Lett.* **2007**, *98*, 015701.

(28) Herzing, A. A.; Kiely, C. J.; Carley, A. F.; Landon, P.; Hutchings, G. J. *Science* **2008**, *321*, 1331.

(29) Koster, A. M.; Calaminici, P.; Casida, M. E.; F-Moreno, R.; Geudtner, G.; Goursot, A.; Heine, T.; Ipatov, A.; Janetzko, F.; del Campo, J. M.; Patchkovskii, S.; Reveles, J. U.; Vela, A.; Salahub, D. R. *deMon2k* deMon Developers, 2006.

(30) Perdew, J. P.; Burke, K.; Ernzerhof, M. *Phys. Rev. Lett.* **1996**, *77*, 3865.

(31) (a) Schwerdtfeger, P.; Dolg, M.; Schwarz, W. H. E.; Bowmaker, G. A.; Boyd, P. D. W. *J. Chem. Phys.* **1989**, *91*, 1762. (b) Dolg, M. Effective Core Potentials. In *Modern Methods and Algorithms of Quantum Chemistry*; John von Neumann Institute for Computing: Jülich, 2000; Vol. 1, p 479.

(32) De, H. S.; Krishnamurty, S.; Pal, S. *J. Phys. Chem. C* **2009**, *113*, 7101.

(33) De, H. S.; Krishnamurty, S.; Pal, S. *J. Phys. Chem. C* **2010**, *114*, 6690.

(34) (a) Godbout, N.; Salahub, D. R.; Wimmer, J. A. E. *Can. J. Phys.* **1992**, *70*, 560. (b) Köster, A. M.; Flores-Moreno, R.; Reveles, J. U. *J. Chem. Phys.* **2004**, *121*, 681.

(35) Wells, D. H., Jr.; Delgass, W. N.; Thomson, K. T. *J. Chem. Phys.* **2002**, *117*, 10597.

(36) Hakkinen, H.; Abbet, S.; Sanchez, A.; Heiz, U.; Landman, U. *Angew. Chem., Int. Ed.* **2003**, *42*, 1297.

(37) Gamboa, G. U.; Calaminici, P.; Geudtner, G. G.; Köster, A. M. *J. Phys. Chem. A* **2008**, *112*, 11969.

(38) Giorgio, S.; Cabie, M.; Henry, C. R. *Gold Bull.* **2008**, *41*, 167.

(39) (a) Jeyabharathi, C.; Senthil Kumar, S.; Kiruthika, G. V. M.; Phani, K. L. N. *Angew. Chem., Int. Ed.* **2010**, *49*, 2925. (b) Zanchet, A.; D-Urra, A.; Aguado, A.; Roncero, O. *J. Phys. Chem. C* **2011**, *115*, 47.